

Infectious disease prediction with kernel conditional density estimation

Evan L. Ray^{a*}, Krzysztof Sakrejda^a, Stephen A. Lauer^a, Michael A. Johansson^b and Nicholas G. Reich^a

Creating statistical models that generate accurate predictions of infectious disease incidence over multiple time points is a challenging problem whose solution could benefit public health decision makers. We develop a new approach to this problem using kernel conditional density estimation (KCDE) and copulas. We obtain predictive distributions for incidence in individual weeks using KCDE and tie those distributions together into joint distributions using copulas. This strategy enables us to create predictions for the timing of and incidence in the peak week of the season. Our implementation of KCDE incorporates two novel kernel components: a periodic component that captures seasonality in disease incidence, and a component that allows for a full parameterization of the bandwidth matrix with discrete variables. We demonstrate via simulation that a fully parameterized bandwidth matrix can be beneficial for estimating conditional densities. We apply the method to predicting dengue fever and influenza, and compare to a seasonal autoregressive integrated moving average (SARIMA) model and a previously published generalized linear model for infectious disease incidence known as HHH4. KCDE outperforms the baseline methods for predictions of dengue incidence in individual weeks. KCDE also offers more consistent performance than the baseline models for predictions of incidence in the peak week, and is comparable to the baseline models on the other prediction targets. Using the periodic kernel function led to better predictions of incidence. Our approach and extensions of it could yield improved predictions for public health decision makers, particularly in diseases with heterogeneous seasonal dynamics such as dengue fever. Copyright © 0000 John Wiley & Sons, Ltd.

Keywords: copula, dengue fever, infectious disease, influenza, kernel conditional density estimation, prediction

1. Introduction

With the maturation of digital disease surveillance systems in recent years, accurate and real-time infectious disease prediction has become an achievable goal in many contexts. These predictions provide valuable information to

^aDepartment of Biostatistics and Epidemiology, School of Public Health and Health Sciences, University of Massachusetts, Amherst, 415 Arnold House, 715 N. Pleasant Street, Amherst, MA 01003, USA

^bDengue Branch, Division of Vector-Borne Infectious Diseases, Centers for Disease Control and Prevention, San Juan, Puerto Rico, USA

* Correspondence to: Department of Biostatistics and Epidemiology, School of Public Health and Health Sciences, University of Massachusetts, Amherst, 415 Arnold House, 715 N. Pleasant Street, Amherst, MA 01003, USA. Email: elray@umass.edu

public health officials planning disease prevention and control measures [1]. For example, interventions designed to reduce person-to-person transmission of disease have been associated with diminished outbreak intensity [2]. Accurate predictions can help target such interventions more effectively.

In this work, we use a semi-parametric approach that combines a non-parametric method for conditional density estimation referred to as kernel conditional density estimation (KCDE) with a parametric method for modeling joint dependence structures known as copulas. We apply this method to make predictions for three targets chosen by the CDC as relevant to public health:

1. Incidence h time steps in the future (at “prediction horizon” h).
2. Timing of the peak week of the current season, $w^* \in \{1, \dots, W\}$, where W is the total number of weeks in the season.
3. Binned incidence in the peak week of the current season.

These quantities have emerged as being targets of particular utility in making planning decisions [3, 4].

We model the first of these prediction targets directly; predictions for the second and third prediction targets are derived from a joint predictive distribution of incidence in each remaining week of the season. Using data available up through time t^* , we employ KCDE to obtain separate predictive distributions for disease incidence in each subsequent week of the season. We then combine those marginal distributions using copulas to obtain joint predictive distributions for the trajectory of incidence over the following weeks. Without a technique like copulas to introduce correlation among week-specific predictions the predictions would not realistically represent the time-series nature of infectious disease dynamics. Predictive distributions relating to the timing of, and incidence at, the peak week can be obtained from this joint predictive distribution. Methods combining non-parametric estimates of marginal densities with copulas have been considered previously for other applications such as economic time series [5].

In addition to the novel application of these methods to predicting disease incidence, our contributions include the use of a periodic kernel specification to capture seasonality in disease incidence and a method for obtaining multivariate kernel functions that handle discrete data while allowing for a fully parameterized bandwidth matrix. Previous implementations of kernel methods involving discrete variables have employed a kernel function that is a product of univariate kernel functions [6, 7, 8, 9, 10, 11, 12, 13, 14]. This approach forces the kernel function to be oriented in line with the coordinate axes. Motivated by results showing that multivariate kernel functions with a bandwidth parameterization allowing for flexible orientations can result in improved continuous density estimates [15], we introduce an approach that allows for flexible orientation of discrete kernels by discretizing an underlying continuous kernel function.

In a time-series context, KCDE is a local method in the sense that the density estimate for observations at future time points conditional on covariates is a weighted combination of contributions from previous observations with similar covariate values. Using such local methods is a natural idea in predicting nonlinear systems because it imposes little structure on the assumed relationship between conditioning and outcome variables. The covariates we condition on could include historical observations from the time series we are predicting as well as other variables such as weather or the time of the season.

Applications range from similar infectious disease settings where nearest neighbors regression has been used to make point predictions for incidence of measles [16] and influenza [17] to sports analytics where a version of nearest neighbors regression predicts the career trajectories of current NBA players [18]. We note that KCDE can be seen as a distribution-based counterpart of nearest neighbors regression. For example, the point prediction obtained from nearest neighbors regression is equal to the expected value of the predictive distribution obtained from KCDE if a particular kernel function is used in the formulation of KCDE (e.g., Hastie *et al.* [19] discuss the connection between nearest neighbors and kernel methods for regression).

KCDE has not previously been applied to obtain predictive distributions for infectious disease incidence, but it has been successfully used for prediction in other settings such as survival time of lung cancer patients [9], female labor force participation [9], bond yields and value at risk in financial markets [20], and wind power [21], among others. Similar

methods can also be formulated in the Bayesian framework. For example, Zhou *et al.* [22] model the time to arrival of a disease in amphibian populations using Dirichlet processes and copulas.

There is also a long history of using other modeling approaches for infectious disease prediction, including agent-based models, compartmental models and more generic regression-based time series models such as seasonal autoregressive integrated moving average (SARIMA) models among others. Brown *et al.* [in preparation] and Unkel *et al.* [23] are recent reviews of work on forecasting infectious disease, and describe these alternative approaches in more detail.

Little research has been done comparing the predictive performance of more detailed and disease-mechanistic modeling approaches (agent-based or compartmental models) to more generic models (regression or SARIMA). One difficulty in making comparisons to agent-based models is that these models are often highly parameterized and difficult to independently reproduce or replicate. An additional challenge with agent-based and compartmental models is that expert knowledge is required to tailor them to the specific disease being modeled, and details of the assumed model specification can have a large impact on the quality of predictions [24].

One of the most well-developed modern statistical frameworks for infectious disease prediction is the “HHH4” model [25, 26, 27, 28], a specific variation of a generalized linear model developed for infectious disease. Another commonly used and widely studied approach is the seasonal autoregressive integrated moving average (SARIMA) model. However, both of these approaches have limitations that also hamper generalizability. The HHH4 model specifies a discrete distribution for the observed incidence measure, an appropriate assumption for some data sets, but not for others. The standard SARIMA specification is based on continuous distributions which means that it cannot be directly applied to modeling discrete case count data if low case counts are observed [23].

Several key features distinguish our approach from existing methods commonly used for predicting infectious disease incidence. First, we generate full predictive distributions to fully characterize uncertainty in the predictions. Compared to point predictions, this gives decision makers additional information in situations where the predictive distribution is skewed or has multiple modes. Second, unlike many methods common in the infectious disease literature, KCDE makes minimal assumptions about the underlying system governing disease dynamics. This flexibility makes KCDE suitable for application to a wide variety of time series, including diseases with different latent dynamics. Third, the method can easily be used with either discrete or continuous data by substituting one kernel function specification for another.

One of the few previous methods that shares these characteristics is in Brooks *et al.* [29], who propose an Empirical Bayes method that also gives a joint predictive distribution for incidence in each remaining week in the season. Their approach contrasts with ours in that it takes a “top-down” approach to constructing that predictive distribution, saying that the general trend in incidence over the course of the season will look like a modified version of the season-long trend in incidence from a previous season. On the other hand, the approach we discuss in the present article is a “bottom-up” method that first constructs predictive distributions for incidence in individual weeks and then ties those marginal distributions together to obtain a joint distribution for incidence in all weeks of the season. It seems likely that both of these approaches have something to offer in predicting disease incidence; we will return to this point in the conclusions.

The remainder of this article is organized as follows. First, we describe our approach to prediction using KCDE and copulas. Next, we present the results of a simulation study comparing the performance of KCDE for estimating discrete conditional distributions using a fully parameterized bandwidth matrix and a diagonal bandwidth matrix. We then illustrate our methods by applying them to predicting disease incidence in two data sets: one with a discrete measure of weekly incidence of dengue fever in San Juan, Puerto Rico and a second with a continuous measure of weekly incidence of influenza in the United States. We conclude with a discussion of these results.

2. Method Description

Suppose we observe a measure z_t of disease incidence at evenly spaced times indexed by $t = 1, \dots, T$. Our goal is to obtain predictions relating to incidence after time T using time series of incidence up to time T as well as time series of covariates up to time T .

We allow the incidence measure to be either continuous or discrete and use the term density to refer to either the probability density function or probability mass function as appropriate. We will use a colon notation to specify vectors: for example, $\mathbf{z}_{s:t} = (z_s, \dots, z_t)$. The variable $t^* \in \{1, \dots, T\}$ will be used to represent a time at which we desire to form a predictive distribution, using observed data up through t^* to predict incidence after t^* . When we apply the method to perform prediction for incidence after time T , t^* is equal to T ; however, t^* takes other values in the estimation procedure we describe below.

We introduce the overall structure of our model here and describe its components and parameter estimation in more detail in the following Subsections. At time t^* , our model approximates $f(\mathbf{z}_{(t^*+1):(t^*+H_{t^*})}|t^*, \mathbf{z}_{1:t^*})$ by conditioning only on the time at which we are making the predictions and observed incidence at a few recent time points with lags given by the non-negative integers l_1, \dots, l_M : $f(\mathbf{z}_{(t^*+1):(t^*+H_{t^*})}|t^*, z_{t^*-l_1}, \dots, z_{t^*-l_M})$. For notational simplicity, we take l_M to be the largest of these lags. The model represents this density as follows:

$$f(z_{(t^*+1):(t^*+H_{t^*})}|t^*, z_{t^*-l_1}, \dots, z_{t^*-l_M}) = c^{H_{t^*}} \{f^1(z_{t^*+1}|t^*, z_{t^*-l_1}, \dots, z_{t^*-l_M}; \boldsymbol{\theta}^1), \dots, f^{H_{t^*}}(z_{t^*+H_{t^*}}|t^*, z_{t^*-l_1}, \dots, z_{t^*-l_M}; \boldsymbol{\theta}^{H_{t^*}}); \boldsymbol{\xi}^{H_{t^*}}\}. \quad (1)$$

Here, each $f^h(z_{t^*+h}|t^*, z_{t^*-l_1}, \dots, z_{t^*-l_M}; \boldsymbol{\theta}^h)$ is a predictive density for one prediction horizon obtained through KCDE. The distribution for each prediction horizon depends on a separate parameter vector $\boldsymbol{\theta}^h$. The function $c^{H_{t^*}}(\cdot)$ is a copula used to tie these marginal predictive densities together into a joint predictive density, and depends on parameters $\boldsymbol{\xi}^{H_{t^*}}$. In our applications, we will obtain a separate copula fit for each trajectory length H_{t^*} of interest for the prediction task.

Let W denote the number of time points in a disease season (e.g., $W = 52$ if we have weekly data). For each time t^* , let S_{t^*} denote the time index of the last time point in the *previous* season, so that the times in the same season as t^* are indexed by $S_{t^*} + 1, \dots, S_{t^*} + W$. Finally, let $H_{t^*} = W - (t^* - S_{t^*})$ denote the number of time points after t^* that are in the same season as t^* . H_{t^*} gives the largest prediction horizon for which we need to make a prediction in order to obtain predictions for all remaining time points in the season.

We obtain predictive distributions for each of three prediction targets. We will model the first of these prediction targets directly and frame the second and third as suitable integrals of a predictive distribution $f(\mathbf{z}_{(t^*+1):(t^*+H_{t^*})}|t^*, \mathbf{z}_{1:t^*})$ for the trajectory of incidence over all remaining weeks in the season:

1. Incidence in a single future week with prediction horizon $h \in \{1, \dots, W\}$:

$$f(z_{t^*+h}|t^*, \mathbf{z}_{1:t^*})$$

2. Timing of the peak week of the current season, $w^* \in \{1, \dots, W\}$:

$$P(\text{Peak Week} = w^*) = P(Z_{S_{t^*}+w^*} = \max_w Z_{S_{t^*}+w} | t^*, \mathbf{z}_{1:t^*}) = \int_{\{\mathbf{z}_{(t^*+1):(t^*+H_{t^*})} : z_{S_{t^*}+w^*} = \max_w z_{S_{t^*}+w}\}} f(\mathbf{z}_{(t^*+1):(t^*+H_{t^*})}|t^*, \mathbf{z}_{1:t^*}) d\mathbf{z}_{(t^*+1):(t^*+H_{t^*})}. \quad (2)$$

3. Binned incidence in the peak week of the current season:

$$P(\text{Incidence in Peak Week} \in [a, b]) = P(a \leq \max_w Z_{S_{t^*}+w} < b | t^*, \mathbf{z}_{1:t^*})$$

$$= \int_{\{(\mathbf{z}_{(t^*+1):(t^*+H_{t^*})}) : a \leq \max_w z_{S_{t^*}+w} < b\}} f(\mathbf{z}_{(t^*+1):(t^*+H_{t^*})} | t^*, \mathbf{z}_{1:t^*}) d\mathbf{z}_{(t^*+1):(t^*+H_{t^*})}. \quad (3)$$

In practice, we use Monte Carlo integration to evaluate the integrals in Equations (2) and (3) by sampling incidence trajectories from the joint predictive distribution.

2.1. KCDE for Predictive Densities at Individual Prediction Horizons

We now discuss the use of KCDE to obtain $f^h(z_{t^*+h} | t^*, z_{t^*-l_1}, \dots, z_{t^*-l_M}; \boldsymbol{\theta}^h)$, the predictive density for disease incidence at a particular horizon h after time t^* . To simplify the notation, we define two new variables: $Y_t^h = Z_{t+h}$ represents the prediction target relative to time t , and $\mathbf{X}_t = (t, Z_{t-l_1}, \dots, Z_{t-l_M})$ represents the vector of predictive variables relative to time t . With this notation, the distribution we wish to estimate is $f^h(y_{t^*}^h | \mathbf{x}_{t^*}; \boldsymbol{\theta}^h)$.

To estimate this distribution, we use the observed data to form the pairs (\mathbf{x}_t, y_t^h) for all $t = 1 + l_M, \dots, T - h$ (for smaller values of t there are not enough observations before t to form \mathbf{x}_t and for larger values of t there are not enough observations after t to form y_t^h). We then regard these pairs as a (dependent) sample from the joint distribution of (\mathbf{X}, Y^h) and estimate the conditional distribution of $Y^h | \mathbf{X}$ via KCDE:

$$\hat{f}^h(y_{t^*}^h | \mathbf{x}_{t^*}) = \frac{\sum_{t \in \tau} K^{\mathbf{X}, Y} \{(\mathbf{x}_{t^*}, y_{t^*}^h), (\mathbf{x}_t, y_t^h); \boldsymbol{\theta}^h\}}{\sum_{t \in \tau} K^{\mathbf{X}}(\mathbf{x}_{t^*}, \mathbf{x}_t; \boldsymbol{\theta}^h)} \quad (4)$$

$$= \sum_{t \in \tau} \zeta_{t^*, t}^h K^{Y | \mathbf{X}}(y_{t^*}^h, y_t^h | \mathbf{x}_{t^*}, \mathbf{x}_t; \boldsymbol{\theta}^h), \text{ where} \quad (5)$$

$$\zeta_{t^*, t}^h = \frac{K^{\mathbf{X}}(\mathbf{x}_{t^*}, \mathbf{x}_t; \boldsymbol{\theta}^h)}{\sum_{s \in \tau} K^{\mathbf{X}}(\mathbf{x}_{t^*}, \mathbf{x}_s; \boldsymbol{\theta}^h)}. \quad (6)$$

Here we are working with a slightly restricted specification in which the kernel function $K^{\mathbf{X}, Y}$ can be written as the product of $K^{\mathbf{X}}$ and $K^{Y | \mathbf{X}}$. With this restriction, we can interpret $K^{\mathbf{X}}$ as a weighting function determining how much each observation (\mathbf{x}_t, y_t^h) contributes to our final density estimate according to how similar \mathbf{x}_t is to the value \mathbf{x}_{t^*} that we are conditioning on. These weights are the $\zeta_{t^*, t}^h$ in Equations (5) and (6). $K^{Y | \mathbf{X}}$ is a density function that contributes mass to the final density estimate near y_t^h . The parameters $\boldsymbol{\theta}^h$ control the locality and orientation of the weighting function and the contributions to the density estimate from each observation. In Equations (4) through (6), $\tau \subseteq \{(1 + l_M), \dots, (T - h)\}$ indexes the subset of observations used in obtaining the conditional density estimate; we return to how this subset of observations is defined in the discussion of estimation below.

We take the kernel function $K^{Y, \mathbf{X}}$ to be a product kernel with one component being a periodic kernel in time and the other component capturing the remaining covariates, which are measures of disease incidence:

$$K^{\mathbf{X}, Y} \{(\mathbf{x}_{t^*}, y_{t^*}^h), (\mathbf{x}_t, y_t^h); \boldsymbol{\theta}^h\}$$

$$= K^{\text{per}}(t^*, t; \rho^h, \eta^h) K^{\text{inc}}\{(z_{t^*-l_1}, \dots, z_{t^*-l_M}, z_{t^*+h}), (z_{t-l_1}, \dots, z_{t-l_M}, z_{t+h}); \boldsymbol{\theta}_{\text{inc}}^h\}.$$

Here we have set $\boldsymbol{\theta}^h = (\boldsymbol{\theta}_{\text{per}}^h, \boldsymbol{\theta}_{\text{inc}}^h)$ where $\boldsymbol{\theta}^h$ encompasses parameters both about the periodicity and incidence.

The periodic kernel function was originally developed in the literature on Gaussian Processes [30], and is defined by

$$K^{\text{per}}(t^*, t; \rho^h, \eta^h) = \exp \left[-\frac{\sin^2\{\rho^h(t^* - t)\}}{2(\eta^h)^2} \right]. \quad (7)$$

We illustrate this kernel function in Figure 1. It has two parameters: $\boldsymbol{\theta}_{\text{per}}^h = (\rho^h, \eta^h)$, where ρ^h determines the length of the

periodicity and η^h determines the strength and locality of this periodic component in computing the observation weights $\zeta_{t^*,t}^h$. In our applications, we have fixed $\rho^h = \pi/52$, so that the kernel has period of length 1 year with weekly data. Using this periodic kernel provides a mechanism to capture seasonality in disease incidence by allowing the observation weights to depend on the similarity of the time of year that an observation was collected and the time of year at which we are making a prediction.

The second component of our kernel is a multivariate kernel incorporating all of the other variables in \mathbf{x}_t and y_t^h . In our applications, these variables are measures of incidence; for brevity of notation, we collect them in the column vector $\tilde{\mathbf{z}}_t = (z_{t-l_1}, \dots, z_{t-l_M}, z_{t+h})'$. These incidence measures are continuous in the application to influenza and discrete case counts in the application to dengue fever. In the continuous case, we have used a multivariate log-normal kernel function parameterized in terms of its mode rather than its mean (Figure 1). Using the mode ensures that the contribution to the conditional density is largest near z_{t+h} . This kernel specification automatically handles the restriction that counts are non-negative, and approximately captures the long tail in disease incidence that we will illustrate in the applications Section below. This kernel function has the following functional form:

$$K_{\text{cont}}^{\text{inc}}(\tilde{\mathbf{z}}_{t^*}, \tilde{\mathbf{z}}_t; \mathbf{B}) = \frac{\exp \left[-\frac{1}{2} \{ \log(\tilde{\mathbf{z}}_{t^*}) - \log(\tilde{\mathbf{z}}_t) - \mathbf{B}\mathbf{1} \}' \mathbf{B}^{-1} \{ \log(\tilde{\mathbf{z}}_{t^*}) - \log(\tilde{\mathbf{z}}_t) - \mathbf{B}\mathbf{1} \} \right]}{(2\pi)^{\frac{M+1}{2}} |\mathbf{B}|^{\frac{1}{2}} z_{t^*+h} \prod_{m=1}^M z_{t^*-l_m}} \quad (8)$$

In this expression, $\mathbf{1}$ is a column vector of ones. The matrix \mathbf{B} is a bandwidth matrix that controls the orientation and scale of the kernel function. Subtracting $\mathbf{B}\mathbf{1}$ in the numerator has the effect of placing the mode of the kernel function at z_{t+h} . This bandwidth matrix is parameterized by θ_{inc}^h . In this work we have considered two parameterizations: a diagonal bandwidth matrix, and a fully parameterized bandwidth based on the Cholesky decomposition. To obtain the discrete kernel (Figure 1), we integrate an underlying continuous kernel function over hyper-rectangles containing the points in the range of the discrete random variable (see supplement for details).

We estimate the bandwidth parameters θ^h by numerically maximizing the cross-validated log score of the predictive distributions for the observations in the training data. For a random variable Y with observed value y the log score of the predictive distribution f_Y is $\log\{f_Y(y)\}$. A larger log score indicates better model performance. In obtaining the cross-validated log score for the predictive distribution at time t^* , we leave the year of training data before and after the time t^* out of the set τ in Equations (4) through (6). Our primary motivation for using the log score as the optimization target during estimation is that this is the criteria that has been used to evaluate and compare prediction methods in two recent government-sponsored infectious disease prediction contests [3, 4]. We apply our method to the data sets from those competitions in the applications section below, and report log scores to facilitate comparisons with other results from those competitions that may be published in the future. In general, the log score is a strictly proper scoring rule; i.e., its expectation is uniquely maximized by the true predictive distribution [31]. However, its use as an optimization criterion has been criticised for being sensitive to outliers [31]. In the kernel density estimation literature, this approach to estimation is referred to as likelihood cross-validation, and similar criticisms have been made regarding its performance in handling outliers and estimating heavy-tailed distributions [32, 33]. This is relevant to application of the method to infectious disease prediction, as the distribution of disease incidence tends to be skewed right with a long upper tail. It is possible that the use of cross-validated log scores in estimation could lead to too-large bandwidth estimates, in turn inflating the width of the predictive distribution. We will return to this possibility in our conclusions.

2.2. Combining Marginal Predictive Distributions with Copulas

We use copulas [34] to tie the marginal predictive distributions for individual prediction horizons obtained from KCDE together into a joint predictive distribution for the trajectory of incidence over multiple time points. The copula is a parametric function that captures the dependence relations among a collection of random variables and allows us to compute the joint distribution from the marginal distributions. Figure 16 in the supplement shows that the copula induces

positive correlation in the predictive distributions for incidence in nearby weeks, so that high incidence in one week is more likely to be followed by high incidence in weeks soon after.

To describe our methods for both continuous and discrete distributions, it is most convenient to frame the discussion in this Subsection in terms of cumulative distribution functions (CDF) instead of density functions. We will use a capital C to denote the copula function for CDFs and a lower case c to denote the copula function for densities. Similarly, the predictive densities $f^h(y_{t^*}^h | \mathbf{x}_{t^*}; \boldsymbol{\theta}^h)$ we obtained in the previous Subsection naturally yield corresponding predictive CDFs $F^h(y_{t^*}^h | \mathbf{x}_{t^*}; \boldsymbol{\theta}^h)$.

Our model specifies the joint CDF for $(Y_{t^*}^1, \dots, Y_{t^*}^{H_{t^*}})$ as follows:

$$F^{H_{t^*}}(y_{t^*}^1, \dots, y_{t^*}^{H_{t^*}} | \mathbf{x}_{t^*}; \boldsymbol{\theta}^1, \dots, \boldsymbol{\theta}^{H_{t^*}}, \boldsymbol{\xi}^{H_{t^*}}) = C\{F^1(y_{t^*}^1 | \mathbf{x}_{t^*}; \boldsymbol{\theta}^1), \dots, F^{H_{t^*}}(y_{t^*}^{H_{t^*}} | \mathbf{x}_{t^*}; \boldsymbol{\theta}^{H_{t^*}}); \boldsymbol{\xi}^{H_{t^*}}\} \quad (9)$$

The copula function C maps the marginal CDF values to the joint CDF value. We use the isotropic normal copula implemented in the R [35] package `copula` [36]. The copula function is given by

$$C(u_1, \dots, u_H; \boldsymbol{\xi}^H) = \Phi_{\Sigma^H}(\Phi^{-1}(u_1), \dots, \Phi^{-1}(u_H)), \quad (10)$$

where Φ^{-1} is the inverse CDF of a univariate normal distribution with mean 0 and variance 1 and Φ_{Σ^H} is the CDF of a multivariate normal distribution with mean 0 and covariance matrix Σ^H . The isotropic specification sets $\Sigma^H = [\sigma_{i,j}^H]$, where

$$\sigma_{i,j}^H = \begin{cases} 1 & \text{if } i = j, \\ \xi_d^H & \text{if } |i - j| = d \end{cases} \quad (11)$$

Intuitively, ξ_d^H captures the amount of dependence between incidence levels at future times that are d weeks apart.

We obtain a separate copula fit for each value of H from 2 to W (note that a copula is not required for “trajectories” of length $H = 1$). Broadly, estimation for the model parameters proceeds in two stages: first we estimate the parameters for KCDE separately for each prediction horizon $h = 1, \dots, H$ as described in the previous Section, and second we estimate the copula parameters while holding the KCDE parameters fixed. We give a more detailed description of this estimation procedure in the supplement. In general the two-stage approach may result in some loss of efficiency relative to one-stage methods, but this efficiency loss is small for some model specifications [37]. Also, it results in a large reduction in the computational cost of parameter estimation.

3. Simulation Study

One component of the KCDE model specification outlined in Subsection 2.1 is the parameterization of the bandwidth matrix. We conducted a simulation study to examine the utility of using a fully parameterized matrix specification instead of a diagonal bandwidth matrix when estimating discrete conditional distributions with KCDE. The simulation study is motivated by the simplest case of predicting incidence in a single week using KCDE: predicting incidence at time $t + h$ given incidence at time t . A central characteristic of the disease incidence data we analyze in the next Section is the presence of positive correlation between incidence in nearby time points (Supplemental Figure 2). In this simulation study we demonstrate that in the presence of such correlation, using fully parameterized bandwidth matrices can improve conditional density estimates over using a diagonal bandwidth.

There are many factors that determine the relative performance of KCDE estimators with different bandwidth parameterizations. In this simulation study, we vary just one of these factors: the sample size ($N = 100$ or $N = 1000$). These sample sizes are roughly similar to the number of observations in the training data sets used in the applications in

Section 4 (where we have training sets of size 692 in the application to influenza and 988 in the application to dengue fever).

We conducted 500 simulation trials for each sample size. In each trial, we simulated N observations of a discretized bivariate normal random variable \mathbf{X} with mean $\mathbf{0}$ and covariance matrix Σ where Σ has 1 on the diagonal and 0.9 off of the diagonal (see Supplement for further detail). Using these observations as a training data set, we estimated the bandwidth parameters for two variations on a KCDE model for the conditional distribution of $X_1|X_2$: one with a diagonal bandwidth matrix specification and one with a fully parameterized bandwidth matrix. In this simulation study, the kernel function was obtained by discretizing a multivariate normal kernel function rather than a log-normal kernel function as in the applications below. Otherwise, the method is as described previously.

We evaluated the conditional density estimates by an importance sampling approximation of the Hellinger distance of the conditional density estimate from the true conditional density, integrated over the range of the covariates (see supplement). The Hellinger distance lies between 0 and 1, with smaller values indicating that the density estimate is better. It has been argued that the Hellinger distance is preferred to other measures of the quality of kernel density estimates such as integrated squared error [38]. For each combination of the training set sample size, dimension, and simulation trial, we compute the difference between the Hellinger distance from the true conditional distribution achieved with a diagonal bandwidth matrix and with a fully parameterized bandwidth matrix.

The results indicate that in the presence of correlation between the conditioning variable and the density estimation target, using a fully parameterized bandwidth matrix instead of a diagonal bandwidth generally yields improved density estimates as measured by the integrated Hellinger distance (Figure 2). The average improvement from using a fully parameterized bandwidth matrix is larger with a sample size of $N = 100$ instead of $N = 1000$, but there is also more variation in performance with the smaller sample size. This suggests that using a fully parameterized bandwidth may be helpful in applications similar to infectious disease prediction where there is correlation between the quantity being predicted (e.g., future incidence) and the quantities that we condition on in order to make the predictions.

4. Applications

In this Section, we illustrate our methods through applications to prediction of infectious disease incidence in two examples with real disease incidence data sets. We begin with a discussion of the data, then we describe the models we compare and the evaluation procedures before discussing the results.

4.1. Data

We apply our methods to two infectious disease data sets (Figure 3). The first data set consists of a weekly count of reported cases of dengue fever in San Juan, Puerto Rico. The second data set consists of a composite indicator of flu activity generated by the Centers for Disease Control (CDC) and referred to as the weighted influenza-like illness (wILI) index. The wILI is calculated as the of a proportion of doctor visits with influenza-like illness to clinics participating in the U.S. Outpatient Influenza-like Illness Surveillance Network (ILINet). The measured proportions are weighted by state population and combined into region-level scores. We did not attempt to replicate this weighting scheme and instead used wILI directly in our models. These data sets were used in two recent prediction competitions sponsored by the United States federal government [3, 4].

An important feature of both of these time series is that they exhibit fairly regular seasonal trends: incidence of dengue fever usually reaches a peak during the summer months and a nadir during the winter months, while influenza typically peaks during the winter and reaches a nadir during the summer months. For the purposes of making predictions of seasonal targets with the dengue data, we have used the definition of a season used by the competition administrators: the season begins in the week starting on April 29th or April 30th (depending on the year); historically, this has been the week of the

year with lowest dengue incidence. For the influenza data, we define the season as beginning in the 30th week of the year; which is the week starting on July 29th or July 30th. Again, historically the lowest incidence of influenza has tended to occur near that time.

4.2. Prediction targets and evaluation criteria

We use the three prediction targets described in Section 2 (Supplemental Figure 3). Following the precedent set in the competitions, we make predictions for *binned* incidence in the peak week. For the dengue data set, the bins are $[0, 50)$, $[50, 100)$, \dots , $[500, \infty)$. For the influenza data set, the bins are $[0, 0.5)$, $[0.5, 1)$, \dots , $[13, \infty)$. Our predictions for incidence in individual weeks are for the raw, unbinned, incidence measure.

We divided each data set into two subsets. The last four years of each data set are reserved as a test set for evaluating model performance. The size of the test set was determined by the dengue prediction competition administrators. In the influenza data set, the last four years of data included only observations for three full seasons. The first period is used as a training set in estimating the model parameters. For the influenza data, we had 14 years of training data (1997 through 2010); for the dengue data, we had 19 seasons of training data (1990/1991 through 2008/2009). All predictions are made as though in real time, assuming that once cases are reported they are never revised and that there are no delays in reporting. Specifically, we use only data up through a given week to make predictions for incidence after that week.

We evaluated model performance for predictions in each data set using log scores (log scores were defined previously in Section 2.1). For each season in the testing period, we examined the log scores for predictions made in all weeks of the season, as well as for smaller subsets of those weeks that are most relevant to decision makers using predictions to set public health policy. Specifically, for incidence in individual weeks, we examined model performance for predictions of incidence in the weeks where the eventually observed incidence was at least $2/3$ of the maximum incidence observed in the testing phase. For predictions of incidence in the peak week and the timing of the peak week, we evaluated performance of predictions made before the peak actually occurred. Additionally, for predictions of incidence in individual weeks, we considered the coverage rate of predictive intervals obtained from each method.

4.3. Models

Our applications evaluate four variations on KCDE model specifications:

1. The “Null KCDE” model omits the periodic component of the kernel function and uses a diagonal bandwidth matrix specification for the incidence kernel.
2. The “Full Bandwidth KCDE” model omits the periodic component of the kernel function and uses a fully parameterized bandwidth matrix specification for the incidence kernel.
3. The “Periodic KCDE” model includes the periodic component of the kernel function and uses a diagonal bandwidth matrix specification for the incidence kernel.
4. The “Periodic, Full Bandwidth KCDE” model includes the periodic component of the kernel function and uses a fully parameterized bandwidth matrix specification for the incidence kernel.

We include three baseline models for comparison to our methods. The first is a seasonal autoregressive integrated moving average (SARIMA) model. In fitting this model, we first transformed the observed incidence measure to the log scale (after adding 1 in the dengue data set, which included some observations of 0 cases); this transformation makes the normality assumptions of the SARIMA model more plausible. We then performed first-order seasonal differencing, and obtained the final model fits using the `auto.arima` function in R’s `forecast` package [39]; this function uses a stepwise procedure to determine the terms to include in the model. This procedure resulted in a $\text{SARIMA}(2,0,0)(2,1,0)_{52}$ model for the influenza data and a $\text{SARIMA}(3,0,2)(1,1,0)_{52}$ model for the dengue data. In applying this model to the dengue data, we have discretized the predictive distributions obtained from SARIMA using the same methods that we

used for KCDE. This discretization was not used in model estimation since it is not available in the standard estimation software.

The second baseline model is the “HHH4” model for infectious disease incidence [25, 26, 27], available in the *surveillance* [40] package in R. This is a generalized linear model with either a Poisson or Negative Binomial family. The mean is a linear combination of autoregressive and sinusoidal components. We followed the model selection and estimation procedures outlined in [27] (see Supplement for details). The prediction target for dengue data is discrete case counts and easily implemented in the HHH4 software (Figure 4). The prediction target for flu requested by the CDC is proportion of doctor visits with flu-like illness weighted by state population. Implementing this in HHH4 would require weighting state-level predictions. As we did not attempt to make state level predictions we did not use HHH4 as a reference model for the flu data.

For predictions of peak timing and binned peak incidence, we considered a third naive baseline model that assigned equal probability to all bins (where for peak timing, there is one bin for each week in the season).

4.4. Results

4.4.1. For predictions of incidence in individual weeks, KCDE outperforms the baseline models. KCDE specifications including a periodic kernel component consistently had the highest or close to the highest mean log scores for both data sets whether aggregating across all weeks or only high incidence weeks (Table). Additionally, the worst-case performance of the HHH4 and SARIMA models was much lower than the worst-case performance of any of the KCDE specifications (Table) for all combinations of the data set and the subset of weeks considered.

In the application to dengue fever, KCDE offered the largest improvements relative to the baseline models for predictions in weeks with high incidence near the season peaks (Table ??, Figure 5 and Supplemental Figures 6 through 8). For example, in weeks with more than 184 reported cases (two thirds of the maximum weekly case count in the testing period), the median log score difference between the predictions from the Periodic, Full Bandwidth KCDE model and SARIMA was about 1.48 ($Q_1 = 0.25$, $Q_3 = 2.72$) where values greater than zero show KCDE making more accurate predictions than SARIMA. The median log score difference relative to HHH4 for these weeks was about 0.94 ($Q_1 = 0.41$, $Q_3 = 1.95$). Translating to a probability scale, in these periods of high incidence this KCDE specification assigned about 5 times higher probability to the observed outcome as SARIMA on average and about **1.25** times higher probability as HHH4 on average. Moreover, there were cases where the KCDE model assigned up to about 450 times as much probability to the realized outcome as SARIMA, and over **1300** times as much probability as HHH4. **Across all weeks in the test period and all prediction horizons, neither baseline model ever outperformed this KCDE specification by a factor of more than 9.** Similar patterns also hold with the other KCDE specifications. For the application to influenza, there were not consistent trends in the relative performance of the models in low and high incidence weeks.

In both applications, the predictive intervals for incidence in individual weeks are quite wide for all of the methods we considered (Figure). We evaluated the coverage rates of these intervals. For dengue fever, the coverage rates in the test phase were actually lower than the nominal coverage rate for all methods (Table). However, the KCDE models were generally closer to the target coverage rates than the baseline models, indicating that the width of the predictive intervals from KCDE give an appropriate representation of uncertainty about future dengue incidence. For predictions of influenza, the coverage rates for all KCDE specifications as well as the baseline SARIMA model were too large. For this application, none of the models had consistently better or worse performance than the others as measured by coverage rates of the predictive intervals.

4.4.2. For predictions of peak incidence the KCDE models with periodic kernel components had better mean performance than the baseline models in the application to dengue fever; and in both applications the KCDE models had more consistent performance across seasons than the baseline models (Table, Figure). In the application to dengue fever, the HHH4 model struggled to predict peak incidence in the two test phase seasons with the highest peak, generally performing worse than a

naive approach using equal bin probabilities in those seasons. The SARIMA model did well at predicting peak incidence for dengue, with overall performance that only slightly lower than the Periodic, Full Bandwidth KCDE specification and similar performance in all four test phase seasons. However, in the application to influenza the SARIMA model struggled in the test phase season with highest incidence, with performance levels generally falling below the approach using equal bin probabilities. Meanwhile, the KCDE specifications had much more consistent performance across all test phase seasons, and never did much worse than using equal bin probabilities. For dengue fever the Periodic, Full Bandwidth KCDE specification had the highest average log scores and best worst-case log scores for predictions of peak incidence (Table), while in the application to influenza the KCDE models did only a little worse than SARIMA overall, and did much better in the influenza season with highest incidence.

4.4.3. For predictions of peak week timing made before the peak actually occurred, the KCDE models without periodic kernel components had the best performance in the application to dengue fever, but the SARIMA model had the best performance in the application to influenza. For dengue fever, both the SARIMA and HHH4 models consistently underperformed relative to the naive approach using equal bin probabilities for predictions of peak timing. On the other hand, the KCDE models, and particularly those that did not use a periodic kernel component, generally outperformed this baseline. There was quite a bit of variability in the timing of peak dengue incidence between test phase seasons, and the models including seasonal terms sometimes failed badly when the peak occurred relatively early or late (Figure 6). The KCDE specifications without periodic terms were more robust to this variation in season timing. There was less variability in the timing of the season peak in the three complete test phase seasons in our influenza data, and the SARIMA model was the overall best performing model in that application. However, the SARIMA model was still outperformed by the KCDE models in the influenza season with the latest peak. All methods we evaluated tend to converge rapidly on the truth once the peak week has passed.

4.4.4. In most cases, including a periodic kernel component in the KCDE specification led to improved predictions . KCDE specifications including a periodic kernel component had better average performance than the corresponding KCDE specification without a periodic kernel component for predicting incidence in individual weeks in all combinations of the data sets and the subset of weeks considered. The periodic kernel also led to better predictions of peak incidence in every case except for early season predictions in the application to influenza when the bandwidth matrix for the incidence kernel component was fully parameterized. For predictions of peak timing, including the periodic kernel component was helpful in the application to influenza, but led to worse performance for early-season predictions of the peak timing for dengue incidence.

We have seen that the SARIMA model generally had higher mean performance than the KCDE models in the application to influenza (although it also had less consistent performance for predictions of incidence in individual weeks or at the peak week). We believe that the difference in relative performance of KCDE and the baseline models for prediction in the dengue and influenza data sets can be explained to a great extent by differences in the underlying disease processes and how they relate to the model specifications. The most salient difference between the two time series is the much greater season-to-season variability in the dengue data set relative to the influenza data set (Figure 3). For dengue, the peak incidence in the largest season is about 30 times larger than the peak incidence in the smallest season; this ratio is only about 3 for influenza. It may be the case that the restrictive structure of the SARIMA and HHH4 models means that they are not able to capture the dynamics of dengue incidence accurately. For example, Held and Paul [27] discuss the fact that the seasonal structure in the HHH4 model does not explicitly allow for different amplitudes in different seasons. Relaxing that structure by using a non-parametric approach such as KCDE may yield improved capability to represent the disease dynamics. This is less of an issue in predicting influenza where there is much more consistency across different seasons.

5. Conclusions

Prediction of infectious disease incidence at horizons of more than a few weeks is a challenging task. We have presented a semi-parametric approach to doing this based on KCDE and copulas and found that it is a viable method that can yield improved predictions relative to commonly employed methods in this field. In predicting incidence of dengue fever in individual weeks, our approach offered consistent and substantial performance gains relative to a SARIMA model and the HHH4 model. These improvements were particularly concentrated in the times that are of most interest to public health decision makers: periods of high incidence near the season peak. In the application to influenza, our method did about as well as SARIMA when predicting incidence in individual weeks.

Overall, across both data sets our method offered more consistency than the baseline models in predictions for incidence in the peak week. Both baseline models suffered in one or more seasons with high incidence where they made substantially worse predictions than a naive model assigning equal probability to each incidence bin, whereas KCDE never did much worse than this naive model. For pre-peak predictions of peak week timing, there were multiple seasons where the SARIMA model consistently underperformed relative to the naive approach of assigning equal probability to each week of the year; KCDE and HHH4 were more consistently at or above the level of this naive approach. These improvements in the reliability of early-season predictions are valuable to public health officials planning interventions several weeks or months before the peak of the disease season. However, since year-to-year variation is substantial, continued evaluation of these methods on datasets with longer prospective testing phases could provide better information about long-run performance of all of these methods.

Our implementation of KCDE offers two main methodological contributions. Most importantly in the context of modeling infectious disease, we have introduced the use of a periodic kernel component that captures seasonality. In both of our applications, including this periodic kernel component in the KCDE specification led to substantial improvements in the predictive distributions for incidence in individual weeks. We also introduced a method for obtaining kernel functions that are appropriate for use with discrete data while allowing for a fully parameterized bandwidth matrix. In our applications, using a fully parameterized bandwidth matrix did not lead to consistent improvements in predictions. However, we have demonstrated through a simulation study that the fully parameterized bandwidth can be helpful in some conditional density estimation tasks. This general method for obtaining discrete kernel functions may be beneficial in other applications of KCDE.

A major advantage of the approach we have outlined is its flexibility in terms of cleanly handling both discrete and continuous data and a variety of underlying disease mechanisms. Our method consistently yielded reasonable predictions for all three prediction targets in both applications. As we have seen, the HHH4 model is formulated in terms of discrete case counts and so could not be directly applied to the influenza data where the disease measure was continuous. Even in the data set where it could be used, the HHH4 model underperformed relative to KCDE in predictions for incidence in individual weeks and incidence in the peak week. Similarly, the standard SARIMA model is formulated in terms of continuous distributions. The resulting continuous predictive distributions can be discretized as we have done in this article, but without extra coding effort the method is not appropriate for use with case count data when small integer numbers of cases are reported. Furthermore, our approach consistently equalled or exceeded the performance SARIMA across the applications to dengue and influenza.

There is room for extensions and improvements to the methods we have outlined in this article. One limitation of our work lies in the selection of covariates for the predictive model. We have simply used incidence at the two most recent time points, and possibly the observation time, as covariates. We considered using a stepwise variable selection approach to select the model specification, but we found this to be too computationally expensive to be practical; the full grid search suggested by De Gooijer and Gannoun [41] in similar settings with only one bandwidth parameter would be far too slow for our methods.

Another method for improving our ability to use covariates would be to replace variable selection with shrinkage.

[9] show that when cross-validation is used to select the bandwidth parameters in KCDE using product kernels, the estimated bandwidths corresponding to irrelevant covariates tend to infinity asymptotically as the sample size increases. We conjecture that by introducing an appropriate penalty on the elements bandwidth matrix, bandwidths for irrelevant covariates could be driven to infinity at lower sample sizes. This technique should allow us to include more (possibly irrelevant) covariates in the model. If successful, this would also enable further exploration of using other predictive variables such as weather, incidence measures from neighboring locations, **or data from internet searches and social media** in the model.

In many disease incidence data sets, we observe multiple incidence time series simultaneously. For example, in addition to the national level WILI index used in this article, the influenza-like illness data from the CDC contain measures of incidence for 10 smaller regions within the United States, and break down incidence within four age groups. The methods described in this article could be applied to make predictions with multiple time series. One possible approach to this would be to fit a separate predictive model for each time series, using the other time series as covariates that are conditioned on.

Another aspect of our method that should be explored further is the use of log score in estimation. We used log scores in this work to match the use of log scores in evaluating and comparing the performance of different models. The log score has the advantage of defining a proper scoring rule, but it has the disadvantage of being sensitive to extreme values. Previous authors have suggested the use of other loss functions in estimation for kernel-based density estimation methods that reduce these effects, such as variations on integrated squared error [20] or the continuous ranked probability score [21]. **Despite discussion in the literature of the potential limitations of using log scores for estimation with kernel-based methods, there is not conclusive evidence that use of log scores caused any difficulties in our application. For example, while the predictive interval coverage rates were too high in the application to influenza, coverage rates were too low in the application to dengue fever. Nevertheless, details of the loss function used in estimation could impact the utility of the resulting predictions.**

In the present article, we have simplified the disease prediction task by assuming that the disease incidence measure is reported accurately and without delay. This allowed us to focus on the narrower methodological question of examining whether KCDE is able to capture infectious disease dynamics. However, in order to apply the methods in a real time setting it will be crucial to relax this assumption. We envision two ways that this could be done. First, we could model the relationship between initial reports of incidence and the final revised incidence measure. Using that model, we could use initial reports of incidence at any given time to predict the revised incidence at that time. These predictions of final incidence could then be used as inputs to the KCDE prediction model outlined in this article. This approach is similar in spirit to the methods used by Brooks *et al.* [29]. An alternative approach could use KCDE to directly learn a relationship between initial, unrevised, reports of disease incidence and the final incidence measure in future weeks.

The KCDE modeling framework could also be applied to directly model the joint distribution of incidence in multiple future weeks without the use of a copula. If we were to directly model incidence in all remaining weeks of the season with KCDE the method would operate more similarly to the approach of Brooks *et al.* [29], who directly model the trajectory of incidence over the course of the season. However, we believe that this line would have limited success since fully nonparametric estimation of the joint distribution of incidence in 40 future weeks (for example) given only about 15 to 20 years of past data will be challenging. Another possible approach would be to use KCDE to obtain a joint predictive density of incidence in smaller groups of weeks (for example, 2 - 5 weeks at a time) and then combine those predictive densities using a mechanism such as a copula. Such an intermediate approach might be able to capture more information about medium-term trends in incidence such as holiday effects than the method we have presented in this article without suffering from the curse of dimensionality as much as direct application of KCDE to an entire season at a time.

There is also a long history of using other modeling approaches such as compartmental models for infectious disease

prediction. KCDE is distinguished from these approaches in that it makes minimal assumptions about the data generating process. This can be either an advantage or a disadvantage of KCDE. On the positive side, these minimal assumptions are what make KCDE appropriate for use with a wide variety of disease processes with minimal changes to the model specification. On the other hand, we believe that a well-specified mechanistic model might outperform KCDE in certain circumstances. However, rather than selecting one “preferred” modeling framework or model formulation, we believe it may be fruitful to incorporate the methods developed in this paper as components of an ensemble with several different types of models. An appropriately constructed ensemble incorporating predictions from KCDE as well as other methods might perform better than any of the component models on their own, and would be a valuable approach for maximizing the utility of these predictions to public health decision makers.

6. Software

The estimation methods were implemented in R and C. All source code and data are available in R packages hosted on GitHub [42].

7. Supplementary Material

The reader is referred to the on-line Supplementary Materials for technical details and additional figures with further information about the results.

Acknowledgments

The authors thank the competition administrators for making disease incidence data available. This work was supported by the National Institute of Allergy and Infectious Diseases at the National Institutes of Health (grants R21AI115173 and R01AI102939).

References

1. Manheim D, Chamberlin M, Osoba OA, Vardavas R, Moore M. *Improving Decision Support for Infectious Disease Prevention and Control: Aligning Models and Other Tools with Policymakers' Needs*. RAND Corporation, 2016.
2. Hatchett RJ, Mecher CE, Lipsitch M. Public health interventions and epidemic intensity during the 1918 influenza pandemic. *Proceedings of the National Academy of Sciences* 2007; **104**(18):7582–7587.
3. Pandemic Prediction and Forecasting Science and Technology Interagency Working Group. Dengue Forecasting Jul 2015. [Http://dengueforecasting.noaa.gov/](http://dengueforecasting.noaa.gov/).
4. Epidemic Prediction Initiative. FluSight: Seasonal Influenza Forecasting Jan 2016. [Http://dengueforecasting.noaa.gov/](http://dengueforecasting.noaa.gov/).
5. Patton AJ. A review of copula models for economic time series. *Journal of Multivariate Analysis* 2012; **110**:4–18.
6. Aitchison J, Aitken CG. Multivariate binary discrimination by the kernel method. *Biometrika* 1976; **63**(3):413–420.
7. Bowman AW. A note on consistency of the kernel method for the analysis of categorical data. *Biometrika* 1980; **67**(3):682–684.
8. Grund B. Kernel estimators for cell probabilities. *Journal of Multivariate Analysis* 1993; **46**(2):283–308.
9. Hall P, Racine J, Li Q. Cross-validation and the estimation of conditional probability densities. *Journal of the American Statistical Association* 2004; **99**(468):1015–1026.
10. Hall P, Li Q, Racine JS. Nonparametric estimation of regression functions in the presence of irrelevant regressors. *The Review of Economics and Statistics* 2007; **89**(4):784–789.
11. Li Q, Racine J. Nonparametric estimation of distributions with categorical and continuous data. *Journal of Multivariate Analysis* 2003; **86**(2):266–292.

12. Li Q, Racine JS. Nonparametric estimation of conditional CDF and quantile functions with mixed categorical and continuous data. *Journal of Business & Economic Statistics* 2008; **26**(4):423–434.
13. Ouyang D, Li Q, Racine J. Cross-validation and the estimation of probability distributions with categorical data. *Journal of Nonparametric Statistics* 2006; **18**(1):69–100.
14. Racine J, Li Q, Zhu X. Kernel estimation of multivariate conditional distributions. *Annals of Economics and Finance* 2004; **5**(2):211–235.
15. Duong T, Hazelton ML. Cross-validation bandwidth matrices for multivariate kernel density estimation. *Scandinavian Journal of Statistics* 2005; **32**(3):485–506.
16. Sugihara G, May RM. Nonlinear forecasting as a way of distinguishing chaos from measurement error in time series. *Nature* April 1990; **344**:734–741.
17. Viboud C, Boëlle PY, Carrat F, Valleron AJ, Flahault A. Prediction of the spread of influenza epidemics by the method of analogues. *American Journal of Epidemiology* 2003; **158**(10):996–1006.
18. Silver N. We're predicting the career of every NBA player. Here's how. Oct 2015. <http://fivethirtyeight.com/features/how-were-predicting-nba-player-career/>.
19. Hastie T, Tibshirani R, Friedman J. *The Elements of Statistical Learning*. 2nd edn., Springer Science & Business Media, 2009.
20. Fan J, Yim TH. A crossvalidation method for estimating conditional densities. *Biometrika* 2004; **91**(4):819–834.
21. Jeon J, Taylor JW. Using conditional kernel density estimation for wind power density forecasting. *Journal of the American Statistical Association* 2012; **107**(497):66–79.
22. Zhou H, Hanson T, Knapp R. Marginal Bayesian nonparametric model for time to disease arrival of threatened amphibian populations. *Biometrics* 2015; **71**(4):1101–1110.
23. Unkel S, Farrington C, Garthwaite PH, Robertson C, Andrews N. Statistical methods for the prospective detection of infectious disease outbreaks: a review. *Journal of the Royal Statistical Society: Series A (Statistics in Society)* 2012; **175**(1):49–82.
24. Grad YH, Miller JC, Lipsitch M. Cholera modeling: challenges to quantitative analysis and predicting the impact of interventions. *Epidemiology (Cambridge, Mass.)* 2012; **23**(4):523.
25. Held L, Höhle M, Hofmann M. A statistical framework for the analysis of multivariate infectious disease surveillance counts. *Statistical Modelling* 2005; **5**(3):187–199, doi:10.1191/1471082X05st0980a.
26. Paul M, Held L, Toschke AM. Multivariate modelling of infectious disease surveillance data. *Statistics in Medicine* 2008; **27**(29):6250–6267, doi:10.1002/sim.3440.
27. Held L, Paul M. Modeling seasonality in space-time infectious disease surveillance data. *Biometrical Journal* 2012; **54**(6):824–843.
28. Meyer S, Held L, Höhle M. Spatio-temporal analysis of epidemic phenomena using the R package surveillance. *Journal of Statistical Software* 2016; : (to appear).
29. Brooks LC, Farrow DC, Hyun S, Tibshirani RJ, Rosenfeld R. Flexible modeling of epidemics with an empirical bayes framework. *PLOS Comput Biol* 2015; **11**(8):e1004382.
30. MacKay DJ. Introduction to Gaussian processes. *NATO ASI Series F Computer and Systems Sciences* 1998; **168**:133–166.
31. Gneiting T, Raftery AE. Strictly proper scoring rules, prediction, and estimation. *Journal of the American Statistical Association* 2007; **102**(477):359–378.
32. Schuster EF, Gregory GG. On the nonconsistency of maximum likelihood nonparametric density estimators. *Computer Science and Statistics: Proceedings of the 13th Symposium on the interface*, Springer, 1981; 295–298.
33. Scott DW, Factor LE. Monte Carlo study of three data-based nonparametric probability density estimators. *Journal of the American Statistical Association* 1981; **76**(373):9–15.
34. Nelsen RB. *An introduction to copulas*. Springer Science & Business Media, 2007.
35. R Core Team. *R: A Language and Environment for Statistical Computing*. R Foundation for Statistical Computing, Vienna, Austria 2016. URL <https://www.R-project.org/>.
36. Hofert M, Kojadinovic I, Maechler M, Yan J. *copula: Multivariate Dependence with Copulas* 2015. URL <http://CRAN.R-project.org/package=copula>, r package version 0.999-14.
37. Joe H. Asymptotic efficiency of the two-stage estimation method for copula-based models. *Journal of Multivariate Analysis* 2005; **94**(2):401–419.
38. Kanazawa Y. Hellinger distance and Kullback-Leibler loss for the kernel density estimator. *Statistics & Probability Letters* 1993; **18**(4):315–321.
39. Hyndman RJ. *forecast: Forecasting functions for time series and linear models* 2015. URL <http://github.com/robjhyndman/forecast>, r package version 6.2.
40. Höhle M, Meyer S, Paul M. *surveillance: Temporal and Spatio-Temporal Modeling and Monitoring of Epidemic Phenomena* 2016. URL <https://CRAN.R-project.org/package=surveillance>, r package version 1.12.1.
41. De Gooijer JG, Gannoun A. Nonparametric conditional predictive regions for time series. *Computational Statistics & Data Analysis* 2000; **33**(3):259–275.
42. Ray E, Sakrejda K, Lauer SA, Reich NG. The Reich Lab at UMass-Amherst May 2016. <https://github.com/reichlab/article-disease-pred-with-kcde>.

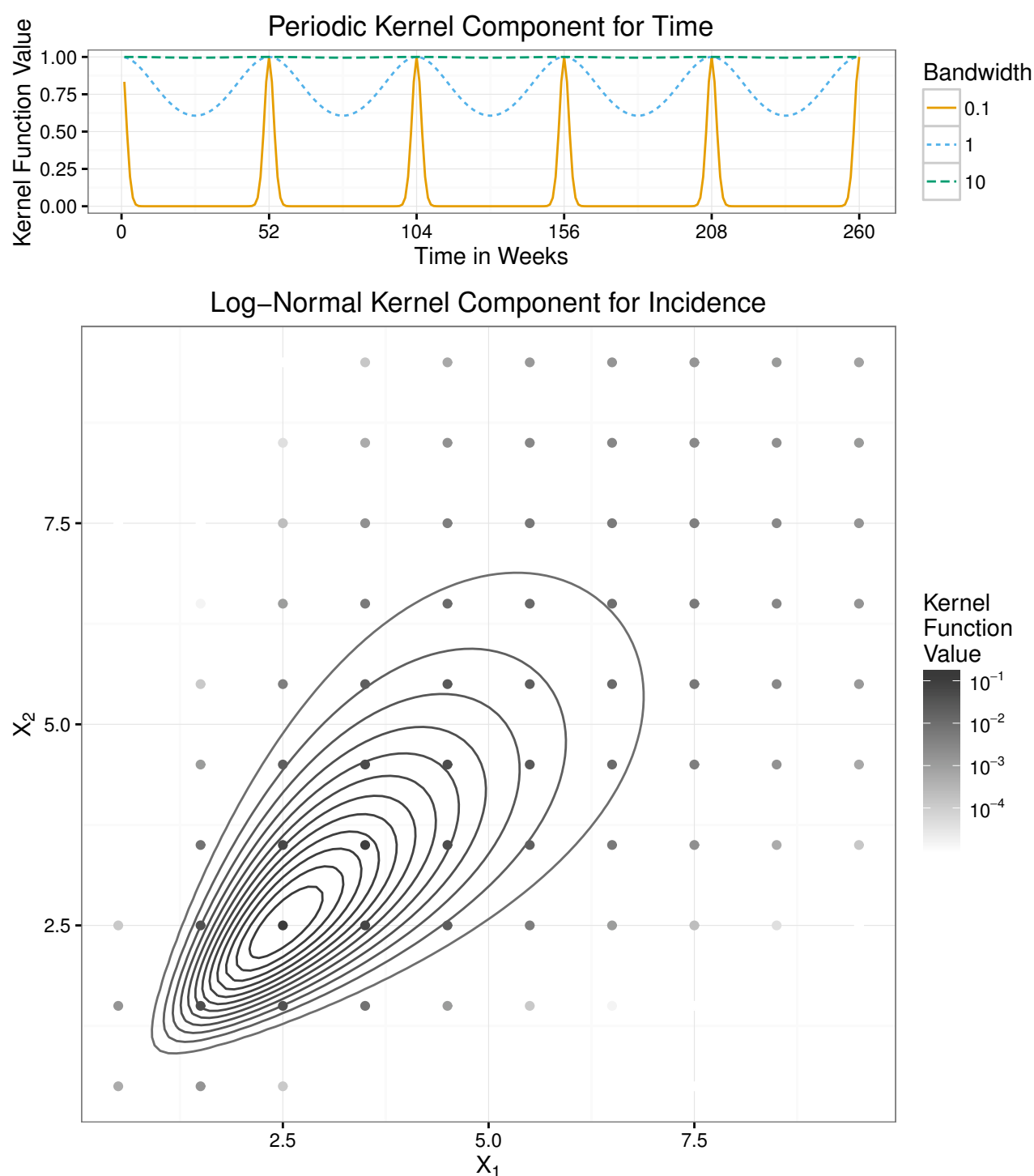


Figure 1. The components of the kernel function. The top panel shows the periodic kernel function illustrated as a function of time in weeks with $\rho = \pi/52$ and three possible values for the bandwidth parameter η . The lower panel shows the log-normal kernel function in the bivariate case. The curves indicate contours of the continuous kernel function and the points indicate the discrete kernel function, which is obtained by integrating the continuous kernel function. The kernel is centered at (2.5, 2.5) and has bandwidth matrix $\begin{bmatrix} 0.2 & 0.15 \\ 0.15 & 0.2 \end{bmatrix}$.

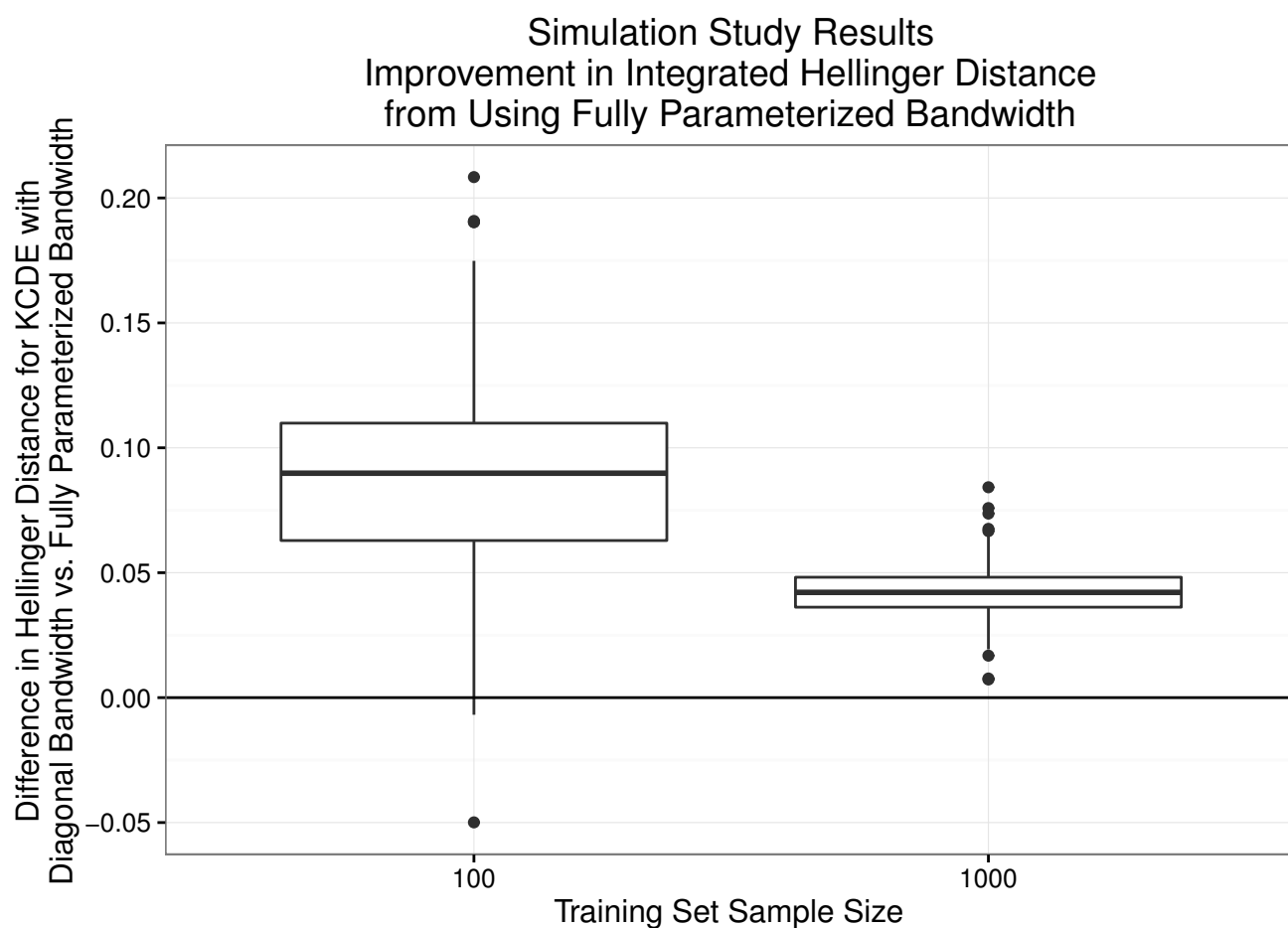


Figure 2. Box plots of results from the simulation study. Positive values indicate simulation trials where the full bandwidth specification outperformed the diagonal bandwidth specification with the same training data set, as measured by Hellinger distance from the target conditional density.

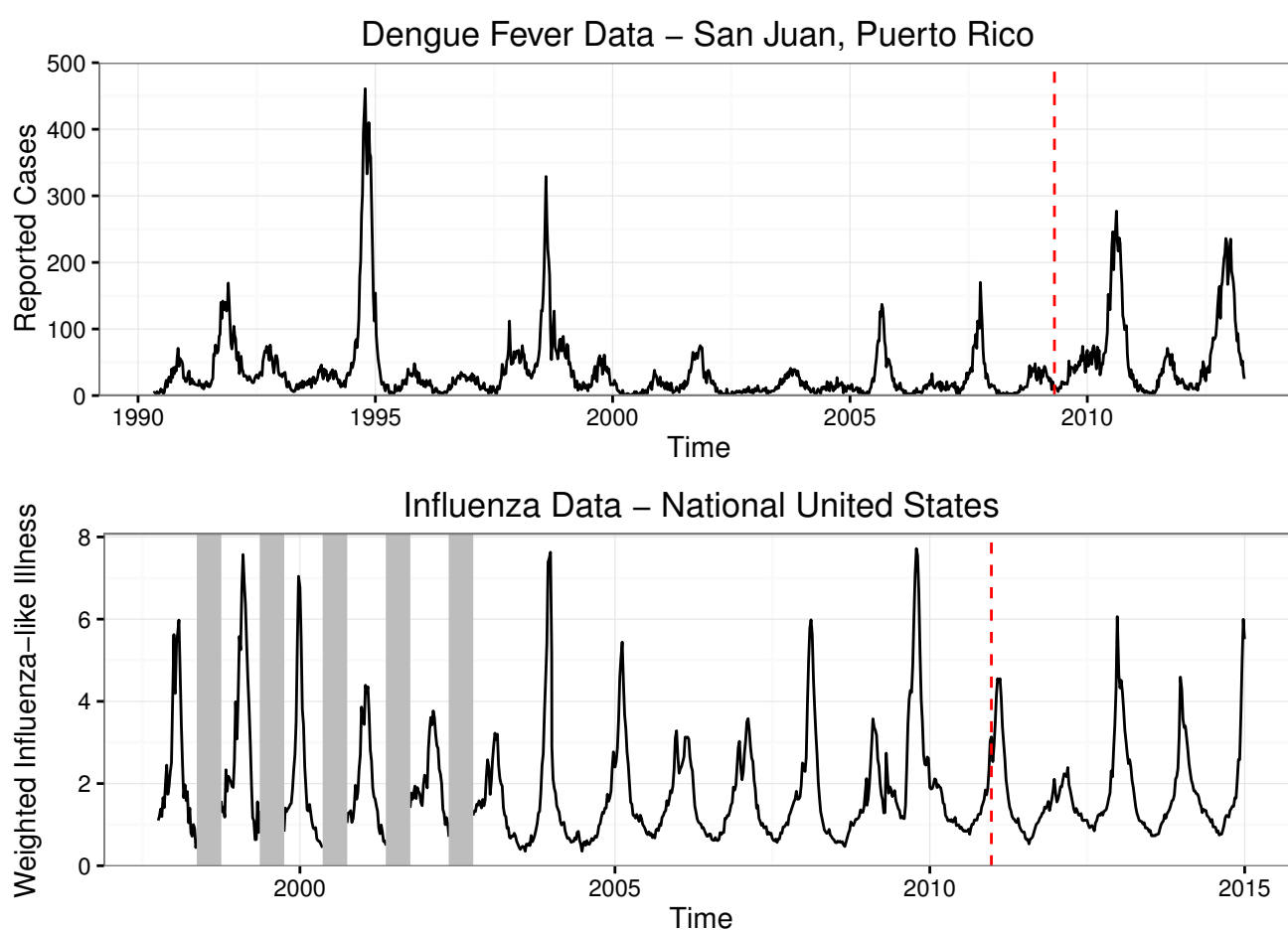


Figure 3. Plots of the data sets we apply our methods to. In each case, the last four years of data are held out as a test data set; this cutoff is indicated with a vertical dashed line. For the flu data set, low-season incidence was not recorded in early years of data collection. These missing data are indicated with vertical grey bars.

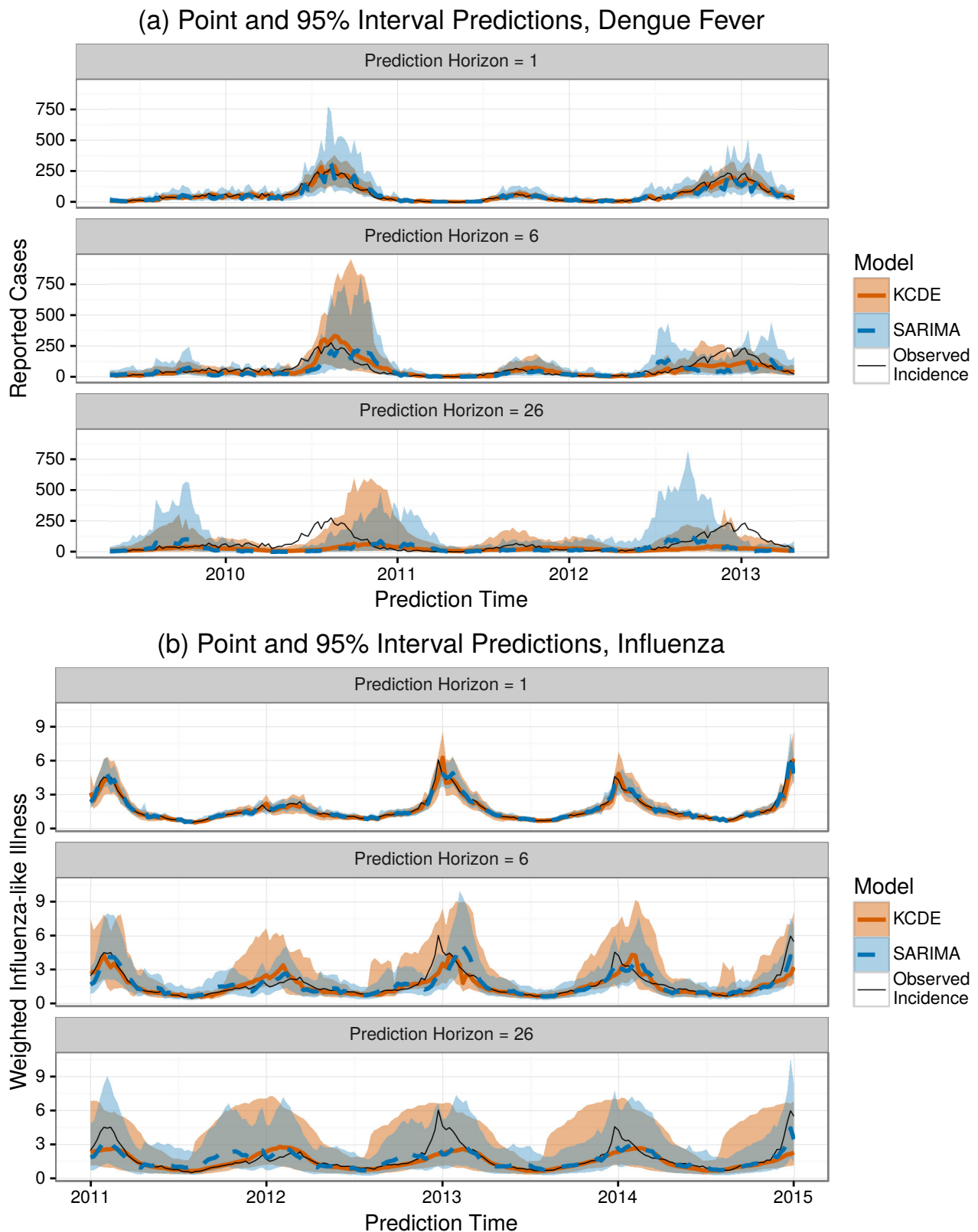


Figure 4. Plots of point and interval predictions from SARIMA and the Periodic, Full Bandwidth KCDE model. The point prediction is the median of the predictive distribution for incidence in the given week. The interval prediction is a percentile interval; for example, the endpoints of the 95% prediction interval are the 2.5th percentile and the 97.5th percentile of the predictive distribution.

Comparison of Periodic, Full Bandwidth KCDE Model and Baseline Models vs. Reported Dengue Cases in Prediction Target Week

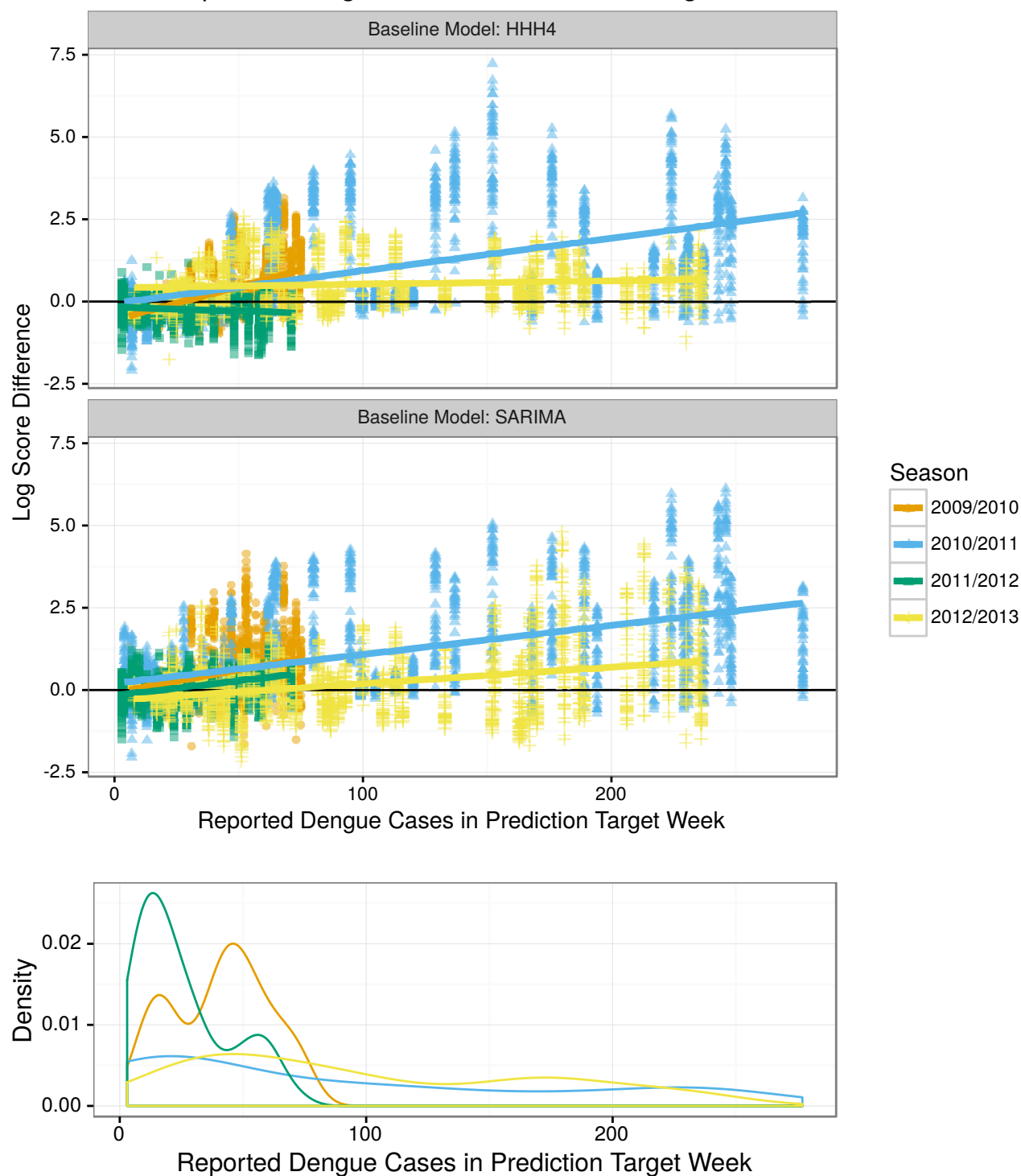


Figure 5. Differences in log scores for the weekly predictive distributions obtained from the Periodic, Full Bandwidth KCDE model and the baseline models, plotted against the observed incidence in the week being predicted. For reference, a log score difference of 2.3 (4.6) indicates that the predictive density from KCDE was about 10 (100) times as large as the predictive density from the baseline model at the realized outcome. Each point corresponds to a unique combination of prediction target week and prediction horizon.

Disease	Model	Target Coverage	Actual Coverage
Dengue	Null KCDE	50	40.96
Dengue	Full Bandwidth KCDE	50	38.79
Dengue	Periodic KCDE	50	44.75
Dengue	Periodic, Full Bandwidth KCDE	50	41.9
Dengue	HHH4	50	40.16
Dengue	SARIMA	50	38.64
Dengue	Null KCDE	95	91.83
Dengue	Full Bandwidth KCDE	95	89.57
Dengue	Periodic KCDE	95	87.34
Dengue	Periodic, Full Bandwidth KCDE	95	86.42
Dengue	HHH4	95	78.22
Dengue	SARIMA	95	79.92
Influenza	Null KCDE	50	69.58
Influenza	Full Bandwidth KCDE	50	70.9
Influenza	Periodic KCDE	50	77.37
Influenza	Periodic, Full Bandwidth KCDE	50	76.15
Influenza	SARIMA	50	73.27
Influenza	Null KCDE	95	99.46
Influenza	Full Bandwidth KCDE	95	99.42
Influenza	Periodic KCDE	95	99.68
Influenza	Periodic, Full Bandwidth KCDE	95	99.48
Influenza	SARIMA	95	99.38

Table 1. Coverage rates for predictions of disease incidence in individual weeks during the test time frame. For each model specification, we have obtained the overall proportion of predictive intervals that contained the realized outcome, combining across all prediction horizons and all times in the test period at which the prediction was made. For each combination of disease and target coverage rate, the result for the model with actual coverage rate closest to the target coverage rate is highlighted.

Disease	Subset	Model	Summary of Log Score Differences					
			Min	Q1	Q2	Mean	Q3	Max
Dengue	All Weeks	Null KCDE	-9.98	-5.86	-4.86	-5.15	-3.91	-1.85
		Full Bandwidth KCDE	-10.37	-5.93	-4.88	-5.16	-3.86	-1.76
		Periodic KCDE	-11.05	-5.87	-4.71	-5.02	-3.82	-1.78
		Periodic, Full Bandwidth KCDE	-10.85	-5.89	-4.72	-5.02	-3.83	-1.68
		<u>HHH4</u>	<u>-16.20</u>	-6.45	-4.65	-5.37	-3.64	-1.75
		SARIMA	-14.42	-6.26	-4.87	-5.46	-3.87	-1.56
	High Incidence	Null KCDE	-9.98	-8.77	-8.45	-8.23	-7.94	-5.33
		Full Bandwidth KCDE	-10.37	-9.07	-8.62	-8.34	-8.03	-5.14
		Periodic KCDE	-11.05	-8.59	-7.91	-7.84	-7.19	-5.26
		Periodic, Full Bandwidth KCDE	-10.85	-8.55	-7.92	-7.79	-7.18	-5.01
		<u>HHH4</u>	<u>-14.66</u>	-10.23	-8.98	-9.05	-7.96	-4.84
		SARIMA	-14.42	-10.62	-9.33	-9.38	-8.02	-5.36
Influenza	All Weeks	Null KCDE	-4.43	-1.37	-0.88	-1.04	-0.57	1.30
		Full Bandwidth KCDE	-5.00	-1.33	-0.78	-0.99	-0.48	1.34
		Periodic KCDE	-3.66	-1.21	-0.50	-0.67	-0.16	1.38
		Periodic, Full Bandwidth KCDE	-3.85	-1.17	-0.48	-0.64	-0.10	1.44
		<u>SARIMA</u>	<u>-6.38</u>	-1.01	-0.52	-0.67	-0.19	1.54
	High Incidence	Null KCDE	-4.43	-3.18	-2.86	-2.89	-2.57	-0.83
		Full Bandwidth KCDE	-5.00	-3.35	-3.03	-3.02	-2.73	-0.67
		Periodic KCDE	-3.66	-2.84	-2.28	-2.40	-1.97	-0.77
		Periodic, Full Bandwidth KCDE	-3.85	-2.90	-2.40	-2.45	-2.03	-0.61
		<u>SARIMA</u>	<u>-6.38</u>	-2.63	-2.19	-2.35	-1.95	-0.37

Table 2. Summaries of model performance for predictions of incidence in individual weeks. The “All Weeks” group summarizes log scores for all combinations of prediction horizon and target week in the test period; the “Low Incidence” group summarizes log scores for predictions of incidence in weeks where the observed incidence was less than one third of the maximum weekly incidence in the test period; the “High Incidence” group summarizes log scores for predictions of incidence in weeks where the observed incidence was at least two thirds of the maximum weekly incidence in the test period. The model in **bold** font had the highest mean log score within each combination of disease and weeks subset. The model in *italicized and underlined* font had the lowest minimum log score within each combination of disease and weeks subset. In some cases, the same model had both the highest average log score and the lowest worst-case log score.

Disease	Subset	Model	Summary of Log Score Differences from Equal Bin Probabilities					
			Min	Q1	Q2	Mean	Q3	Max
Dengue	All Weeks	Null	-0.82	1.35	1.75	1.42	2.17	2.40
		Full Bandwidth	-0.84	1.31	1.80	1.46	2.24	2.40
		Periodic	-0.64	1.38	2.18	1.63	2.39	2.40
		Periodic, Full Bandwidth	-0.40	1.36	2.19	1.66	2.40	2.40
		<u>HHH4</u>	<u>-2.42</u>	1.72	2.15	1.50	2.38	2.40
		SARIMA	-0.69	1.12	1.83	1.56	2.35	2.40
	Before Peak	Null	-0.82	-0.28	1.40	0.83	1.68	2.06
		Full Bandwidth	-0.84	-0.16	1.34	0.87	1.73	2.10
		Periodic	-0.64	-0.06	1.49	1.08	1.88	2.38
		Periodic, Full Bandwidth	-0.40	0.04	1.50	1.12	1.96	2.40
		<u>HHH4</u>	<u>-2.42</u>	-0.73	1.73	0.80	2.03	2.34
		SARIMA	-0.69	0.29	1.32	1.04	1.72	2.37
	All Weeks	Null	-0.19	0.64	1.85	1.87	3.14	3.30
		Full Bandwidth	-0.19	0.83	2.07	1.98	3.18	3.30
		Periodic	-1.23	0.80	2.64	1.96	3.24	3.30
		Periodic, Full Bandwidth	-1.38	0.85	2.77	1.98	3.27	3.30
		<u>SARIMA</u>	<u>-2.42</u>	1.53	3.06	2.16	3.30	3.30
		Before Peak	-0.19	0.47	0.64	0.76	0.79	1.89
Influenza	All Weeks	Null	-0.19	0.64	1.85	1.87	3.14	3.30
		Full Bandwidth	-0.19	0.83	2.07	1.98	3.18	3.30
		Periodic	-1.23	0.80	2.64	1.96	3.24	3.30
		Periodic, Full Bandwidth	-1.38	0.85	2.77	1.98	3.27	3.30
		<u>SARIMA</u>	<u>-2.42</u>	1.53	3.06	2.16	3.30	3.30
		Before Peak	-0.19	0.47	0.64	0.76	0.79	1.89
	Before Peak	Null	-0.19	0.47	0.64	0.76	0.79	1.89
		Full Bandwidth	-0.19	0.56	0.83	0.93	1.27	2.41
		Periodic	-1.23	0.02	0.80	0.78	0.94	2.95
		Periodic, Full Bandwidth	-1.38	0.19	0.85	0.82	1.04	3.07
		<u>SARIMA</u>	<u>-2.42</u>	0.61	1.53	1.11	1.90	3.25
		Before Peak	-0.19	0.47	0.64	0.76	0.79	1.89

Table 3. Summaries of model performance relative to a naive approach assigning equal probability to all bins for predictions of incidence in the peak week. Each row summarizes the differences in log score for the given model and the log score that would be achieved by using equal bin probabilities; positive values indicate that the model performed better than using equal bin probabilities. The “All Weeks” group summarizes results for all combinations of target week in the test period and prediction horizon; the “Before Peak” group summarizes results for predictions in weeks before the actual peak for the given season. The model in **bold** font had the highest mean log score within each combination of disease and weeks subset. The model in *italicized and underlined* font had the lowest minimum log score within each combination of disease and weeks subset. In some cases, the same model had both the highest average log score and the lowest worst-case log score.

Disease	Subset	Model	Summary of Log Score Differences from Equal Bin Probabilities					
			Min	Q1	Q2	Mean	Q3	Max
Dengue	All Weeks	Null	-1.35	0.29	1.18	1.81	3.64	3.95
		Full Bandwidth	-1.33	0.28	1.14	1.83	3.69	3.95
		Periodic	-1.73	0.00	1.55	1.84	3.94	3.95
		<u>Periodic, Full Bandwidth</u>	<u>-3.87</u>	0.03	1.58	1.75	3.95	3.95
		HHH4	-0.92	-0.10	1.33	1.83	3.91	3.95
		SARIMA	-3.65	-0.48	2.27	1.65	3.81	3.95
	Before Peak	Null	-1.35	-0.01	0.31	0.30	0.71	1.96
		Full Bandwidth	-1.33	-0.10	0.30	0.29	0.73	1.71
		Periodic	-1.73	-0.61	0.13	0.19	0.94	2.22
		<u>Periodic, Full Bandwidth</u>	<u>-3.87</u>	-0.73	0.08	0.01	0.63	2.16
		HHH4	-0.92	-0.30	-0.09	0.13	0.49	2.15
		SARIMA	-3.65	-1.62	-0.25	-0.05	1.39	2.76
Influenza	All Weeks	<u>Null</u>	<u>-0.42</u>	1.04	1.64	2.26	3.75	3.95
		Full Bandwidth	-0.24	0.98	1.77	2.24	3.80	3.95
		Periodic	-0.28	1.14	2.20	2.38	3.88	3.95
		Periodic, Full Bandwidth	-0.33	1.03	1.65	2.35	3.92	3.95
		SARIMA	0.08	1.80	3.24	2.69	3.95	3.95
	Before Peak	<u>Null</u>	<u>-0.42</u>	0.70	1.04	0.94	1.30	1.64
		Full Bandwidth	-0.24	0.48	0.98	0.86	1.21	1.85
		Periodic	-0.28	0.74	1.14	1.01	1.38	2.20
		Periodic, Full Bandwidth	-0.33	0.55	1.03	0.95	1.40	1.65
		SARIMA	0.08	0.29	1.80	1.57	2.91	3.34

Table 4. Summaries of model performance relative to a naive approach assigning equal probability to all bins for predictions of the peak week timing. Each row summarizes the differences in log score for the given model and the log score that would be achieved by using equal bin probabilities; positive values indicate that the model performed better than using equal bin probabilities. The “All Weeks” group summarizes results for all combinations of target week in the test period and prediction horizon; the “Before Peak” group summarizes results for predictions in weeks before the actual peak for the given season. The model in **bold** font had the highest mean log score within each combination of disease and weeks subset. The model in italicized and underlined font had the lowest minimum log score within each combination of disease and weeks subset. In some cases, the same model had both the highest average log score and the lowest worst-case log score.

Summary of Results for Peak Week Incidence and Timing

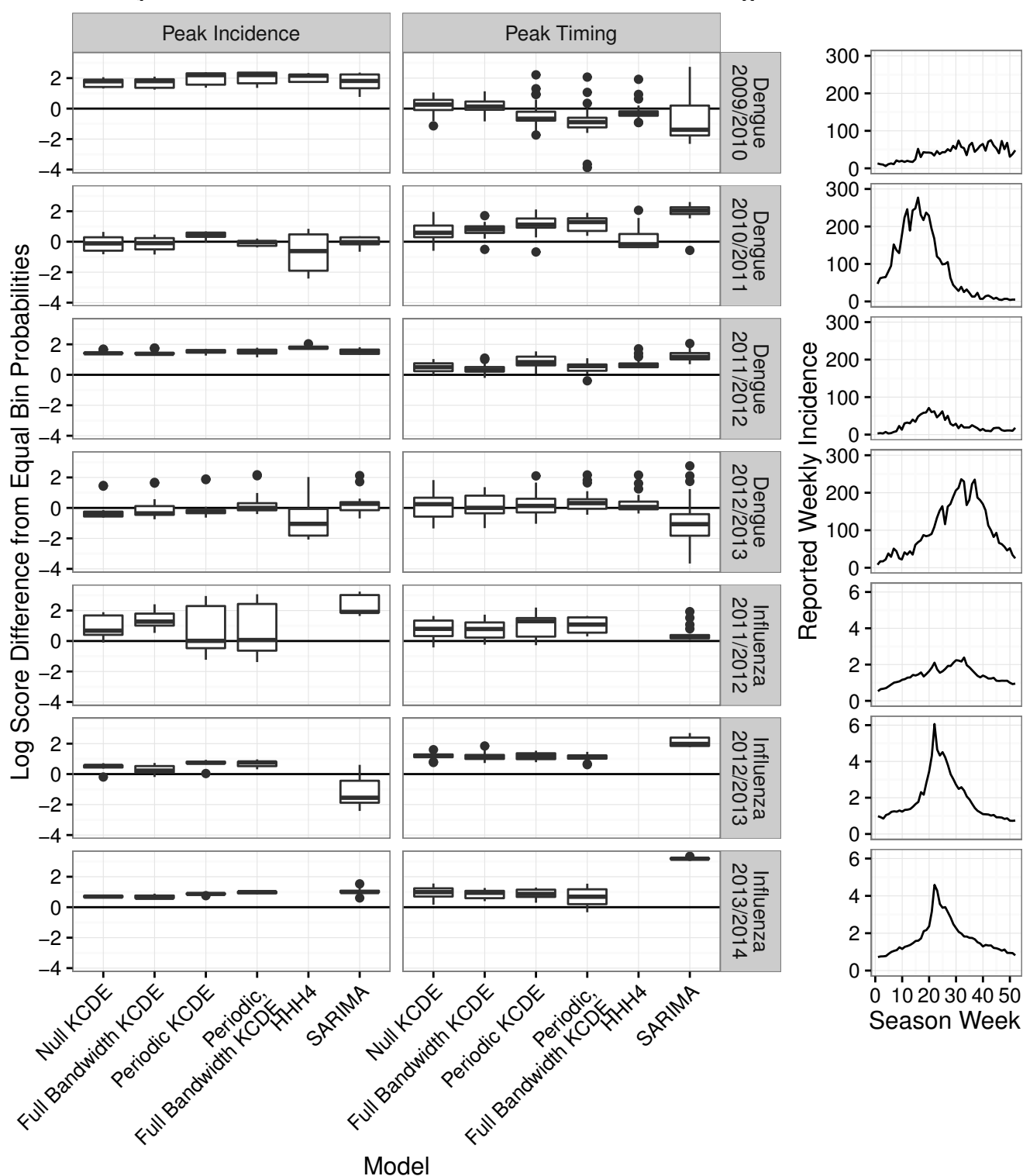


Figure 6. A summary of performance of each method for predicting peak week timing. Each boxplot summarizes all predictions made by a method in a given season in weeks before the actual peak week for that season. The vertical axis is the difference in log scores between the given method and a naive approach assigning equal probability to each week of the year. Positive values indicate cases when the method did better than using equal bin probabilities. The plots on the right display the trajectory of incidence over each season.